

EFFECT OF CONTROL MODE AND TEST RATE ON THE MEASURED FRACTURE TOUGHNESS OF ADVANCED CERAMICS

Bronson D. Hausmann
Case Western Reserve University
Cleveland, Ohio, 44106

Jonathan A. Salem
NASA Glenn Research Center
Cleveland, Ohio, 44135

ABSTRACT

The effects of control mode and test rate on the measured fracture toughness of ceramics were evaluated by using chevron-notched flexure specimens in accordance with ASTM C1421. The use of stroke control gave consistent results with about 2% (statistically insignificant) variation in measured fracture toughness for a very wide range of rates (0.005 to 0.5 mm/min). Use of strain or crack mouth opening displacement (CMOD) control gave ~5% (statistically significant) variation over a very wide range of rates (1 to 80 $\mu\text{m}/\text{m}/\text{s}$), with the measurements being a function of rate. However, the rate effect was eliminated by use of dry nitrogen, implying a stress corrosion effect rather than a stability effect. With the use of a nitrogen environment during strain controlled tests, fracture toughness values were within about 1% over a wide range of rates (1 to 80 $\mu\text{m}/\text{m}/\text{s}$). CMOD or strain control did allow stable crack extension well past maximum force, and thus is preferred for energy calculations. The effort is being used to confirm recommendations in ASTM Test Method C1421 on fracture toughness measurement.

KEY TERMS: CHEVRON-NOTCHED BEAM, FRACTURE TOUGHNESS, SILICON NITRIDE, STRESS CORROSION

NOMENCLATURE

CMOD = Crack mouth opening displacement

LPD = Load point displacement

PID = Proportional-Integral-Derivative feedback loop

P_{max} = Maximum force at failure

INTRODUCTION

Fracture toughness is a critical structural design parameter and an excellent metric to rank materials. It determines fracture strength in the presence of flaws, both inherent and induced, and defines the endpoint of the slow crack growth curve. For design of aerospace structures, quality measurements are required for exposures to environments ranging from high vacuum and low temperature (e.g. the International Space Station) to high humidity and high temperature (e.g. a Florida launch pad). While an excellent standard on fracture toughness measurement of ceramics has been developed by ASTM Test Method C1421, the range of effects necessary for some applications merit further investigation¹. Particularly, measurements on glass-ceramics or glasses are desired. Common concerns include test humidity and test rate^{2,3}. A secondary aspect of test rate is the control mode used.

Rate of force application and test environment have a strong effect on the measured strength and fracture toughness of ceramics and glasses⁴. This is a result of several factors including stress corrosion² and energy stored and released from the test system². Brittle ceramics susceptible to environmental stress corrosion have also been found to exhibit rate-dependent fracture toughness (see Table I). Stress corrosion can be mitigated via dry environments and rapid rates, leaving only stability effects as the prominent concern for fracture toughness measurements.

Stored energy release can be controlled by ensuring crack growth stability. Achieving this stability depends on competing variables such as a stiff load train and a sufficiently sensitive force transducer. In some cases, researchers have resorted to using high capacity (low resolution) force transducers relative to measurements (1% of capacity)⁵, raising metrological concerns.

PROCEDURE

In this work, the effects of control mode, test rate, and environment on the fracture toughness of ceramics were measured by using chevron-notched flexure specimens in accordance with ASTM Test Method C1421¹. The effects of humidity and test rate can be confounded, so to distinguish which factors influenced the results, strain control mode tests were employed over a wide range of rates (1 to 80 $\mu\text{m}/\text{m}/\text{s}$) in both lab air and nitrogen.

In addition to recording strain, CMOD was recorded using a laser micrometer, which measured the displacement between two parallel silicon carbide pins (see fig. 1) fixed to either side of the notch opening. Back face strain, which is linearly proportional to CMOD in the linear elastic region, was sufficient for confirming stable crack extension well past peak force. This was vital for comparison between lab air and dry nitrogen environment tests, because containing the nitrogen prevented use of the laser during testing.

For ease of comparison, fracture toughness values were normalized to the fracture toughness measured when testing at 0.05 mm/min in stroke control. This is a typical testing condition, making it ideal for comparison in terms of percent deviation between various testing configurations (see Table II and fig. 2)⁶.

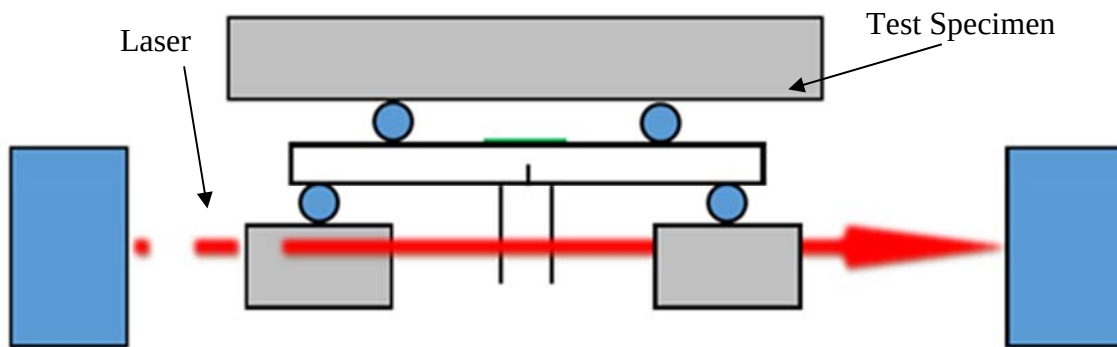


Figure 1. Schematic of the CMOD laser micrometer setup. The laser passes over two thin silicon carbide pins perpendicular to the crack opening. The detector on the right side of the test specimen measures the distance between the pins, outputting the measurement at a rate of about 100 Hz.

RESULTS

It was found that with a low capacity force transducer, four-point flexure, and strain control, consistent results occur over a wide range of rates, particularly when environmental effects are

minimized (see Table II and fig. 2). When environmental effects are present, the difference is less than 7% for an extremely wide range of strain rates. Also noteworthy is that *in situ* toughened silicon nitride is sensitive to stress corrosion, as shown in Figure 3, with the effect on measured fracture toughness being small (<3% variation) for reasonable experiment setups. Use of stroke control, which is less stable, best mitigates the effects occurring in lab air (see Table II and fig. 4) and gives very consistent results.

Strain control tests in lab air show a significant variation in fracture toughness; however, when similar testing is done in dry nitrogen, the trend is significantly reduced (see fig. 5 and 6, respectively). This implies a stress corrosion effect from humidity in the air as opposed to a rate effect from stored energy or other mechanisms. Test repeatability was confirmed by similar force-strain curves as well as sufficient unloading after peak force before failure of the sample. CMOD controlled testing lacked the repeatability of strain control testing due to loop tuning difficulty (fig. 7). This is seen in the curve's unstable appearance beyond peak load. Further refinement of CMOD testing is left to future work.

While CMOD control allowed for asymptotic unloading, the unstable appearance of the unloading curve indicates strain energy was wasted on cyclic unloading. The feedback loop had difficulty remaining closed. Similar repeatability issues were seen in high rate tests performed in dry nitrogen by using strain control. Strain control was stable until low force (10% of maximum), when it typically became unstable. It is suspected that highly concentrated stress fields on strain gages near failure result in this instability. Although it was difficult to control tests from the CMOD channel, CMOD data were recorded during a number of tests. As long as stable crack growth was achieved, force plotted as a function of CMOD decays asymptotically, allowing for future energy calculations (see fig. 8).

Table I. Fracture Toughness of ALSIMAG 614 Alumina.

Stroke Rate	Fracture Toughness by Test Environment (K_{Ivb} (A) MPa \sqrt{m}): Mean \pm S.D. (sample size)		
	Water	Air	Silicone Oil or Dry N ₂
0.05 mm/min	2.75 \pm 0.01 (4)	3.19 \pm 0.07 (7)	3.37 \pm 0.05 (4)
0.01 mm/min	2.64 \pm 0.06 (3)	2.93 \pm 0.10 (3)	3.39 \pm 0.02 (2)

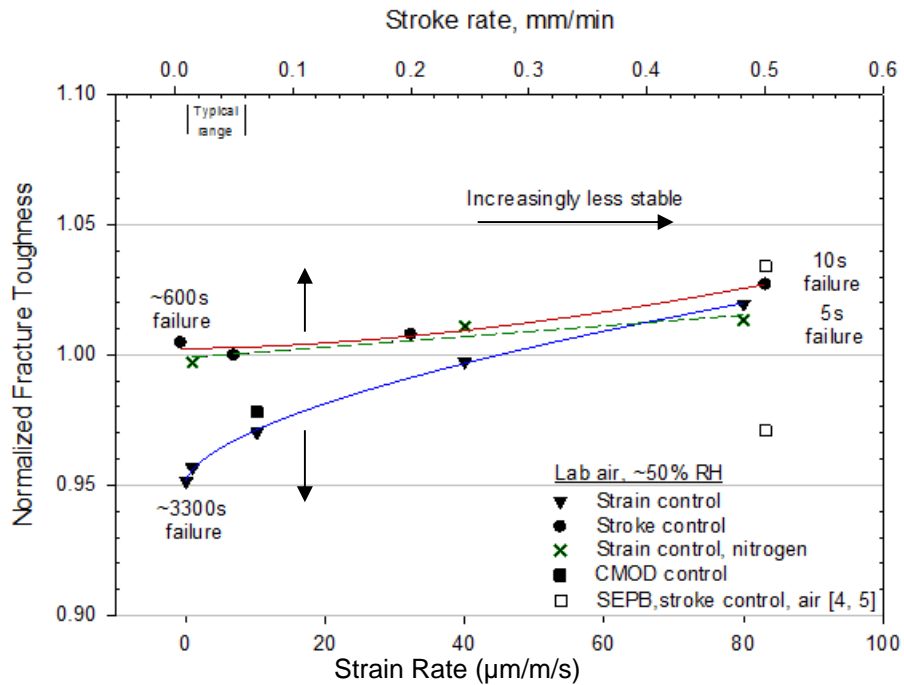


Figure 2. Rate effects for AS800 Silicon Nitride. The upper x axis corresponds to the upper (red) curve, while the lower (blue and green) curves correspond to the lower axis. CMOD control test rate has been converted to a microstrain rate for direct comparison (see Appendix). Values are plotted as deviations from the average test performed at 0.05 mm/min. SEPB data bounds adapted from references 7 and 8.

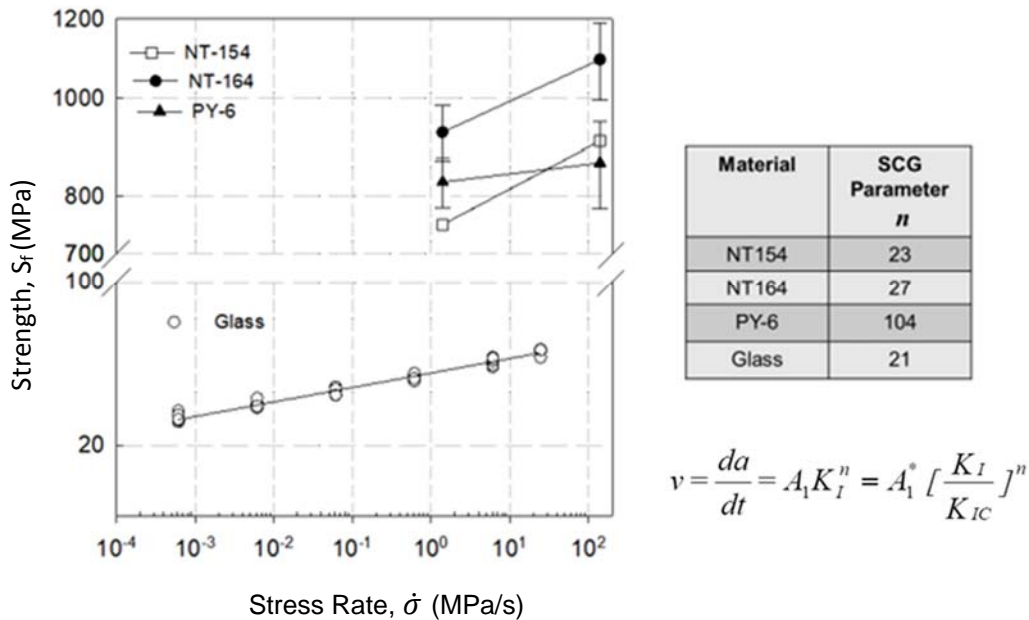


Figure 3. Constant stress rate curves for several silicon nitrides and glass. Slow crack growth parameter n is similar in some nitrides to silicate glass, implying a stress corrosion effect. Adapted from reference 9.

Table II. Fracture Toughness of AS800 Silicon Nitride.

<i>Testing Environment</i>	<i>Testing Mode and Rate (number of tests)</i>	<i>Fracture Toughness, K_{Ivb} (MPa\sqrt{m}) \pmS.D.</i>	<i>Deviation from Typical Test (0.05 mm/min)</i>	<i>Nominal time to peak load (s)</i>
<i>Lab Air</i>	<i>Stroke Control</i>			
	0.005 mm/min	7.87 \pm 0.05	+0.48%	600
	0.05 mm/min	7.83 \pm 0.16	---	100
	0.2 mm/min	7.89 \pm 0.09	+0.7%	20
	0.5 mm/min	8.04 \pm 0.04	+2.7%	10
	<i>Strain Control</i>			
	0.1 μ m/m/s	7.45 \pm 0.15	-4.8%	3300
	1 μ m/m/s	7.49 \pm 0.28	-4.4%	300
	10.25 μ m/m/s	7.60 \pm 0.22	-3.0%	50
	40 μ m/m/s	7.81 \pm 0.10	-0.03%	10
	80 μ m/m/s	7.98 \pm 0.13	+1.96%	5
	<i>CMOD Control</i>			
	0.04 μ m/m/s	7.66 \pm 0.45	-2.3%	50
<i>Dry Nitrogen</i>	<i>Strain Control</i>			
	1 μ m/m/s	7.81 \pm 0.18	-0.03%	300
	40 μ m/m/s	7.95 \pm 0.12	+1.0%	10
	80 μ m/m/s	7.94 \pm 0.59	+1.3%	5
All Data	---	7.79 \pm 0.19	-0.05%	---

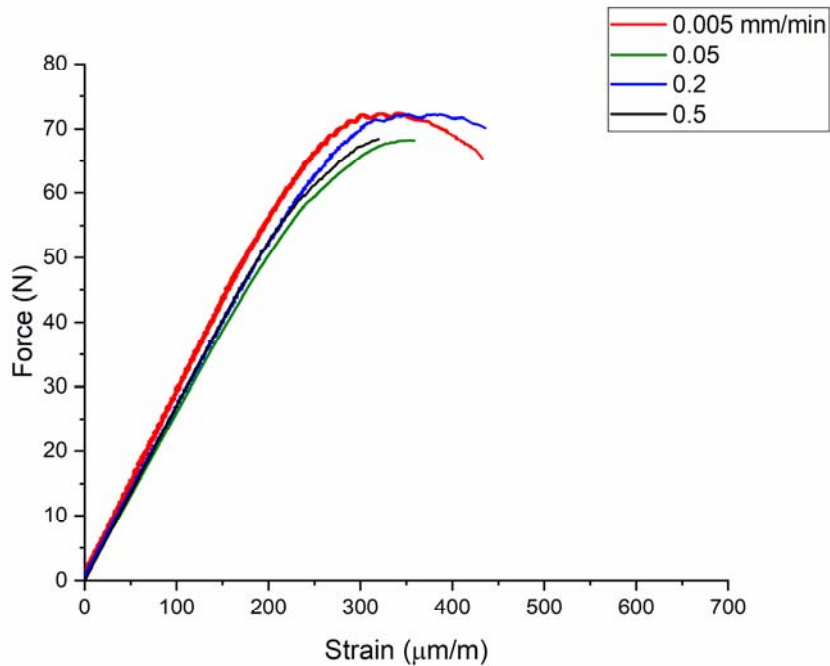


Figure 4. Stroke rate testing representative curves. Force as a function of back face strain for stroke control. Stability is generally improved by testing at a slower rate. 0.05 mm/min is a typical testing rate, allowing for slight crack extension beyond peak force.

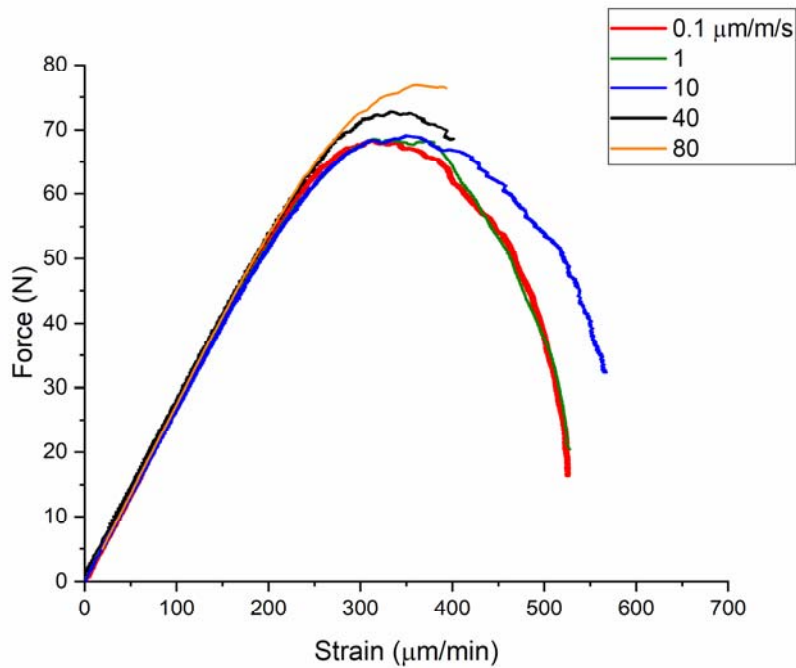


Figure 5. Strain Rate Testing Representative Curves. Force as a function of back face strain, tested in strain control. A marked improvement in stability over stroke rate control testing is exhibited, while still demonstrating instability at higher strain rates.

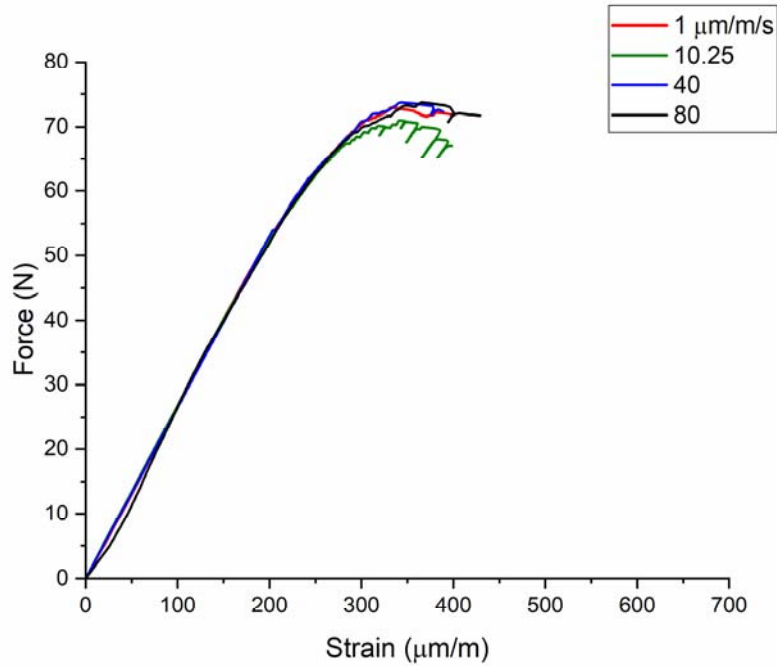


Figure 6. Strain Rate Testing in Dry Nitrogen. Force as a function of back face strain, tested in strain control. Little variation can be seen between testing rates. Some unloading was typical at 10.25 us/s which was likely a result of feedback loop difficulties during crack growth.

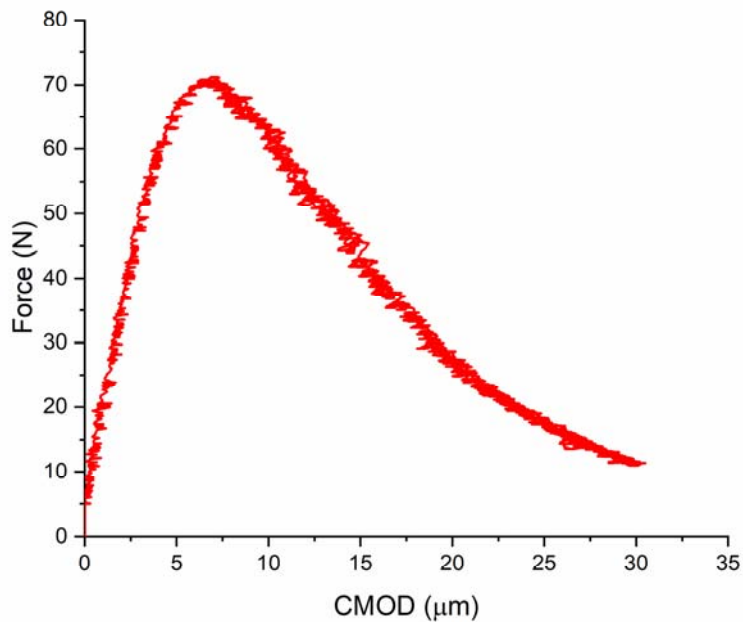


Figure 7. CMOD Rate Testing Representative Curve. Force as a function of CMOD, tested in CMOD control. What appears to be noise in the signal is suspected to be wandering caused by poor feedback loop communication. Most if not all CMOD control tests were able to unload beyond peak force at the cost of data precision.

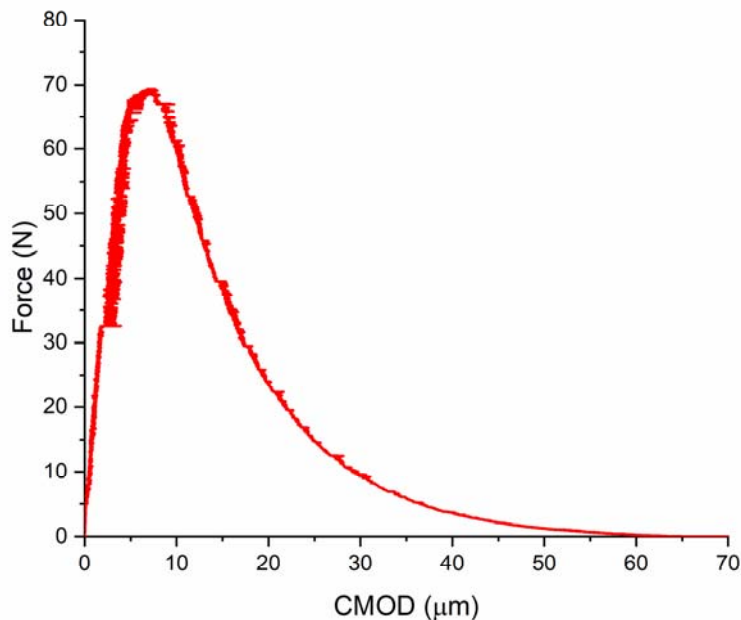


Figure 8. Force as a function of CMOD for CMOD control. The laser micrometer is able to record CMOD data even in strain control. When test specimens exhibit full crack extension through failure, they produce curves that asymptotically approach zero force when plotted as a function of CMOD.

CONCLUSIONS

The fracture toughness of test specimens tested in stroke control was relatively unaffected by rate variations. Stability beyond maximum force, however, was greatly reduced in this mode, leading to failure within 100 microstrain of peak load. Strain controlled testing was able to achieve fully asymptotic failure in some cases, often reaching as low as 20% of peak force before breaking. Test specimens tested in strain control additionally exhibited stress corrosion behavior in a lab air environment, which was confirmed through testing in dry nitrogen. This resulted in a fracture toughness reduction of about 5% for very slow test rates. For engineering purposes, tests performed within 10 to 15 seconds result in comparable fracture toughness regardless of test mode. A compromise must be found between test stability and environmental effects.

Future data processing involving calculation of work of fracture and strain energy release rate could be useful to directly compare control modes. Before this is possible, however, a conversion between load point displacement (LPD) and CMOD must be obtained either experimentally or through finite element analysis. Future work will also include dynamic fatigue testing to confirm that the effect demonstrated in AS800 silicon nitride is due to slow crack growth.

APPENDIX: LINEAR CORRELATION OF CMOD AND BACK FACE STRAIN

CMOD and back face strain were linearly correlated using a strain gauge in tandem with a laser micrometer. By matching the strain channel to a predetermined waveform, a fit was generated that provided direct conversion between the two parameters (see fig. 9). Obtaining this data experimentally allowed for a conversion factor tailored to the exact billet of material as well as the

exact load frame configuration, all without needing to resort to finite element analysis estimates. Similar methods can be employed to correlate LPD to CMOD, and thus to back face strain.

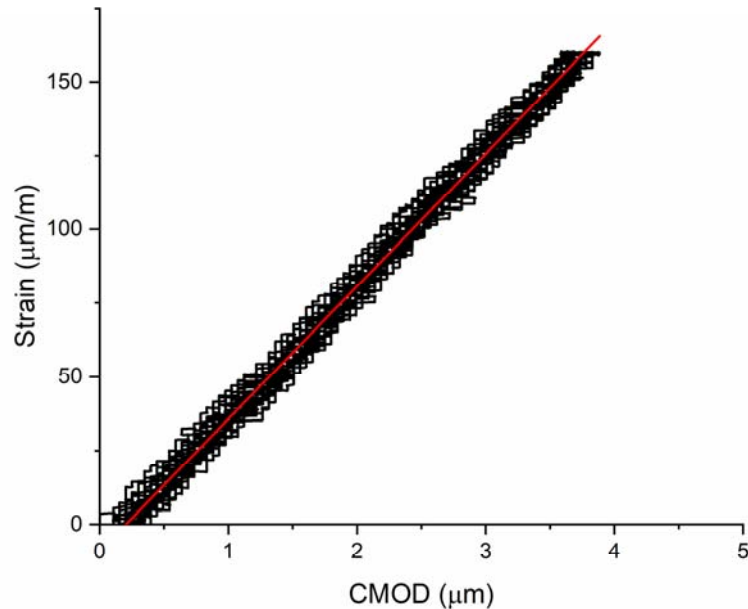


Figure 9. Linear Correlation between CMOD and Back Face Strain for AS800 silicon nitride. The relationship was determined by overlaying several linear loading/unloading cycles and plotting a linear regression for the entire data set.

ACKNOWLEDGMENTS

Bronson Hausmann thanks NASA GRC for its support through the LERCIP project, as well as Dr. Jon Salem for years of collaboration and mentorship.

REFERENCES

¹ ASTM C1421-15, Standard Test Methods for Determination of Fracture Toughness of Advanced Ceramics at Ambient Temperature, Annual Books of ASTM Standards, Vol. 15.01. ASTM International, West Conshohocken, PA. 2018

² J. E. Ritter, "Predicting lifetimes of materials and material structures," *Dental Materials*, vol. 11, no. 2, pp. 142–146, Mar. 1995.

³ S. M. Wiederhorn, "Subcritical Crack Growth in Ceramics," in *Fracture Mechanics of Ceramics*, Springer, Boston, MA, 1974, pp. 613–646.

⁴ S. W. Freiman, S. M. Wiederhorn, and J. Mecholsky John J., "Environmentally Enhanced Fracture of Glass: A Historical Perspective," *Journal of the American Ceramic Society*, vol. 92, no. 7, pp. 1371–1382, Jul. 2009.

- ⁵ Garcia-Prieto, A., Hernandez, J., Lopez, M., and Baudin, C., “Controlled fracture test for brittle ceramics,” *Journal of Strain Analysis*, vol. 46, 2011, pp. 27–32.
- ⁶ Salem, Jonathan; Ghosn, Louis; Jenkins, Michael; Quinn, George. (2008). “Stress Intensity Factor Coefficients for Chevron-Notched Flexure Specimens and a Comparison Fracture Toughness Methods.” *Ceram. Eng. Sci. Proc.* 20. 503 - 512.
- ⁷ Choi, S.R.; Pereira, M.J. et al. “Foreign Object Damage Behavior of Two Gas-turbine Grade Silicon Nitrides by Steel Ball Projectiles at Ambient Temperature,” NASA TM 20020082954, August 2002.
- ⁸ J. A. Salem, “Transparent Armor Ceramics as Spacecraft Windows,” *Journal of the American Ceramic Society*, vol. 96, no. 1, pp. 281–289, Jan. 2013.
- ⁹ Graves, G.A.; Hecht, N.L. “Effects of environment on the mechanical behavior of high-performance ceramics.” Report UDR-TR-94-136. 1995.